PCCP

Accepted Manuscript

ROYAL SOCIETY OF CHEMISTRY

www.rsc.org/pccp

Cite this: DOI: 10.1039/c0xx00000x

www.rsc.org/xxxxxx

COMMUNICATION

The mechanism of Controllable dehydrogenation: CPMD study of the decomposition of $M(BH_4)_x(NH_3)_y$ (M=Li, Mg)

Kun Wang[*a,c], Jian-Guo Zhang[*b], Xu-Qiang Lang[d]

Received (in XXX, XXX) XthXXXXXXXXX 2015, Accepted Xth XXXXXXXXX 2015

DOI: 10.1039/C000000x

Amine metallic borohydrides are synthesized as a new series of hydrogen-storage materials. Their dehydrogenation can be controlled if we choose appropriate centre metals. It's a typical example that $LiBH_4NH_3$ (ALB) and $Mg(BH_4)_2(NH_3)_2$ (AMgB) adopt same symmetries but show totally different appearances in the corresponding decompositions. Both ALB and AMgB are relatively new compounds designed as candidates for solid-state hydrogen storage. In this study, we have applied car-parrinello molecular dynamic (CPMD) method to simulate their overall processes of their decompositions to figure out the mechanisms behind the appearances. The polarization of Mg^{2+} is almost two times larger than that of Li^+, making the Mg^{2+} bond with nitrogen and boron stronger compared to that of Li^+, which improve the appearance of dehydrogenation of AMgB than that of ALB.

Hydrogen resource is the most abundant and clean resource with a high energy content, which make it be a promising alternative energy carrier[1-8]. Ammine metallic borohydrides (AMB) are a series of solid-state hydrogen storage compounds with high percentage of available hydrogen emerged as attractive candidates of new energy resources recently[9-13]. As we studied before[14], the dehydrogenation properties of AMBs can be tuned by changing different centre metals to improve the efficiency of dehydrogenation process or purity of released hydrogen. Most recently, two new monometallic AMBs, $Mg(BH_4)_2(NH_3)_2$ (AMgB)[9] and $LiBH_4NH_3$(ALB)[15] have been synthesized where their structures are similar and they adopt the same symmetries. However, their appearances of dehydrogenation are rather different. AMgB releases almost pure hydrogen in the decomposition (25 ~ 400 ºC)[9] but ALB starts to release ammonia at around 40 ºC[15]. Additionally, the capacity of hydrogen evolution is increased accompanied with a decreased ammonia release capacity after heating ALB to 280 ºC[16].No experiments show the mechanisms behind the interesting appearances. We want to find the reasons of the huge differences between ALB and AMgB although both the two compounds appears similar compositions, geometric structures and symmetries and how the thermal motion triggers their decompositions when increasing the temperature.

The objectives of this study are to characterize the total dissociation processes of the solidate ALB and AMgB by using Car-Parrinello molecular dynamic methods[17] with the plane wave and ultrasoftpseudopotential[18-19]. The optimization and the analysis of electronic structures were implemented in CASTEP program[20]. In the optimization, the Brillouin-zone integration of AMgB and ALB were done by using 3×6×6 and 7×9×3 Monkhorst-Pack meshes[21]. All the kinetic calculations were performed with Quantum Espresso package[22]. The generalized gradient approximation[23] of Perdew, Burke and Erzerhof[24] (GGA-PBE) for the exchange-correlation function has been used throughout. The Vanderbilt-type ultrasoft pseudopotentials[25] with valence states Li ($1s^22s^1$), Mg($2p^63s^2$), B($2s^22p^1$), N($2s^22p^3$) and H($1s^1$) were used to describe the core electrons. A plane wave basis set with an energy cutoff of 500 eV has been used. Structural relaxations of atomic positions, cell shapes and cell volume were carried out by BFGS method[26] until the residual forces and stresses were less than 0.005 eV/Å and 0.01Gpa. The optimized structures are showed in Figure 1.We also studied the total and partial density of states of ALB and AMgB which showed in SI-Figure S1.

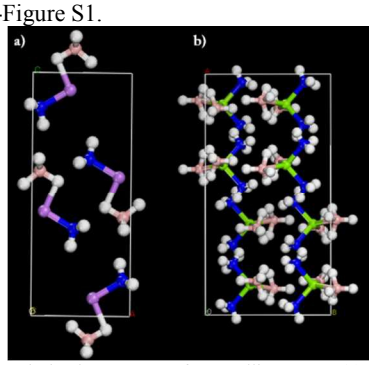

Figure 1. The optimized structure of crystalline ALB (a) and AMgB (b). Theoretical bond length [Å] of ALB: Li-B 2.48 (2.52), N-H 1.03 (1.17), B-H 1.22 (0.95), Li-N 2.04 (2.01), NH-HB 2.25 (2.55). Theoretical bond length [Å] of AMgB: Mg-B 2.41 (2.33), N-H 1.03 (1.00), B-H 1.24 (1.20), Mg-N 2.15 (2.03), NH-HB 2.22 (2.19). The results in the brackets are from the experiments [9, 15]. Purple: Li, green: Mg, blue: N, pink: B, white: H.

ALB adopts orthorhombic symmetry in space group *Pnma*, where *a*= 5.90 Å, *b*=4.48 Å, *c*=14.52 Å. In the crystalline ALB (Figure 1(a)), each Li^+ is tetrahedrally coordinated by one $[BH_4]^-$ group through H^+ and one $[NH_3]$ group through N, with bond angles N-Li-H(B) of 97.70°. Li, N, and B atoms (2 cells in Figure 1(b))are almost aligned in the same [100] plane. The structure of AMgB is similar with that of ALB, which also adopts

Cite this: DOI: 10.1039/c0xx00000x

www.rsc.org/xxxxxx

COMMUNICATION

orthorhombic symmetry but in space group *Pcab*, where *a*= 18.07 Å, *b*=9.43 Å, *c*=8.72 Å. The calculated band gaps of ALB and AMgB are 5.72 eV and 6.0 eV, respectively, which indicates that both of them are wide band-gap insulators. It also means that AMgB is most likely more stable than that of ALB because of its larger band gap. The total and partial density of states have been showed in supporting information.

In order to study the decomposition mechanisms of ALB and AMgB, we applied Car-Parrinello molecular dynamic methods to simulate their proceedings. The total lengths of simulation were 21 ps (210000 steps) for ALB and 8 ps (80000 steps) for AMgB by using the same time step of 4 a.u. The fictitious electron mass is tested as 300 a.u for ALB and 400 a.u for AMgB. Electronic orbital were expanded in a plane wave basis set using an electron density cutoff 400 Ry for both them. The oscillation frequency of the nose thermostat[27] is set as 750 THz. An NVT ensemble was employed for both the simulations.

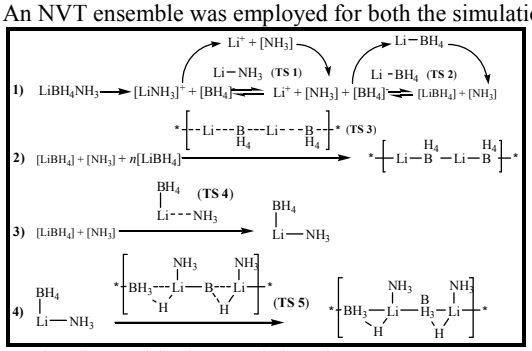

Figure 2. The scheme of the deammoniation of ALB.

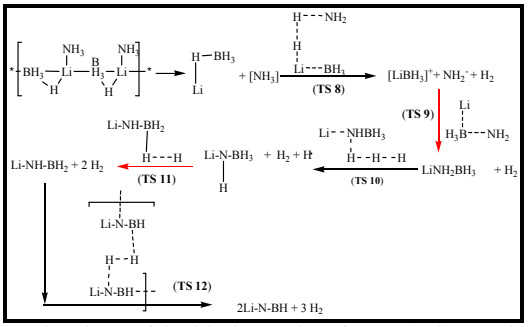

Figure 3. The scheme of the dehydrogenation of ALB. (Red arrows highlight the dehydrogenation at high temperature theoretically)

After convergence of wave function and optimization, the external temperature was gradually increased by an increment of 100 K from 100 to 900 K for ALB and from 100 to 600 K for AMgB. The high temperature is set for accelerating the decomposition. The simulation period at each temperature was 10000 ~30000 steps (1 ~ 3 ps) to make sure it is long enough to avoid sudden and rapid increase of velocity due to fast heating. The relationship between the temperature and the steps' setting is list in the Table S1.

Many transient structures exist only in tens of femtoseconds in the processes. We prefer centring on the transition states or intermediates, which can explain us a 'clear' pathway of the decomposition. The details (the structures of transition states and the corresponding time they first appear) of the decompositions are listed in supplementary information (Table S2 and S3). Both of the decompositions start with the motions of $[NH_3]$ groups away from the molecular ALB and AMgB. The typical pathways of deammoniation and dehydrogenation of ALB and AMgB are showed in Figure 2 to Figure 5. The overall decomposition schemes for ALB and AMgB are showed in Figure S2 and S3.

For the deammoniation of ALB, the bond length of Li-N in $[Li(NH_3)]^+$ elongates from 2.02 Å to 2.08 Å to form a 3-component system consisted of Li^+, $[NH_3]$ and $[BH_4]^+$ around 0.245 ps (**TS1**). Then the 3-component system transforms to the 2-component system comprised of $LiBH_4$ and NH_3(**TS2**). It's a reversible reaction between the 3-component system and the 2-component system, which lasts 16.458 ps (78 % of the total simulation time). It's a enough long period for the liberation of ammonia. So it's the reason why ALB releases ammonia at the beginning of the decomposition.

As for AMgB, there is also a reversible transformation between a similar 3-component system (Mg^{2+}, $[NH_3]$ and $[BH_4]^+$) and the 2-component system ($Mg(BH_4)_2$ and NH_3) at the time of 3.331 ps in the simulation. The balance between **TS1'** and **TS2'**only lasts 0.665 ps, and then it turns back to the original structure of molecular AMgB. The longest bond distance of Mg-N in **TS1'** is 2.23Å, while the longest bond distance of Mg-B in **TS2'** is 2.53 Å. Compared with ALB, the very short time (0.83 % of the total simulation time) of the transformation of AMgB makes a great improvement in controlling the ammonia liberation.

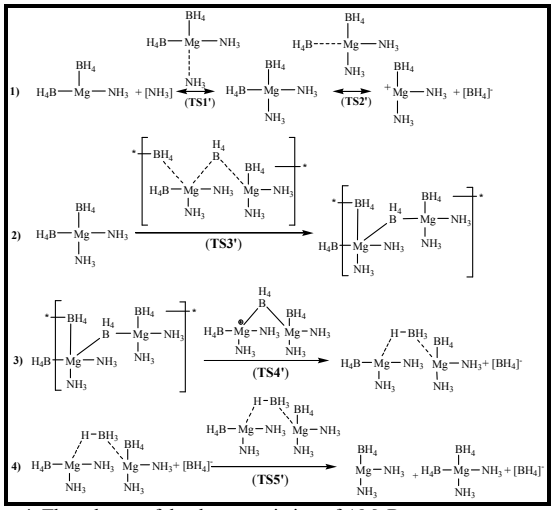

Figure 4. The scheme of the deammoniation of AMgB.

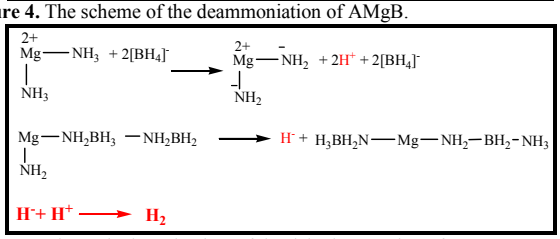

Figure 5. The typical mechanism of the dehydrogenation of AMgB.

The first dehydrogenation of ALB and AMgB are similar with each other. Both of the molecules polymerize firstly (**TS3**$^{(')}$-**TS5**$^{(')}$) and then dehydrogenate. For ALB, during the period of 16.773 ps to 17.54 ps, $H^{\delta+}$ from $[NH_3]$ groups attacks the $H^{\delta-}$ of LiH to release the first molecular hydrogen (**TS8**). After that, the neighbouring molecular fragments of $[NH_2]^-$ and $[LiBH_3]^+$move

Cite this: DOI: 10.1039/c0xx00000x

www.rsc.org/xxxxxx

COMMUNICATION

close to each other to form a structure of $LiNH_2BH_3$ at 17.309 ps (**TS9**). Then the generation of different hydrogen free radicals (**TS10**) caused by arising the temperature, •H(N) separates from nitrogen atom firstly to move forward to •H(B) to form a second molecular hydrogen at 18.28 ps (**TS11**). The third molecular hydrogen is released at 19.8825 ps. So, actually, from 17.309 ps to the end, the last two dehydrogenation steps of ALB are following the decomposition mechanisms of lithium amidoborane ($LiBH_2NH_3$) [28]. The formation of the large amount of hydrogen free radicals which is consistent with the truth[16]that dehydrogenation of ALB requires high temperature (280 ºC in the experiment).

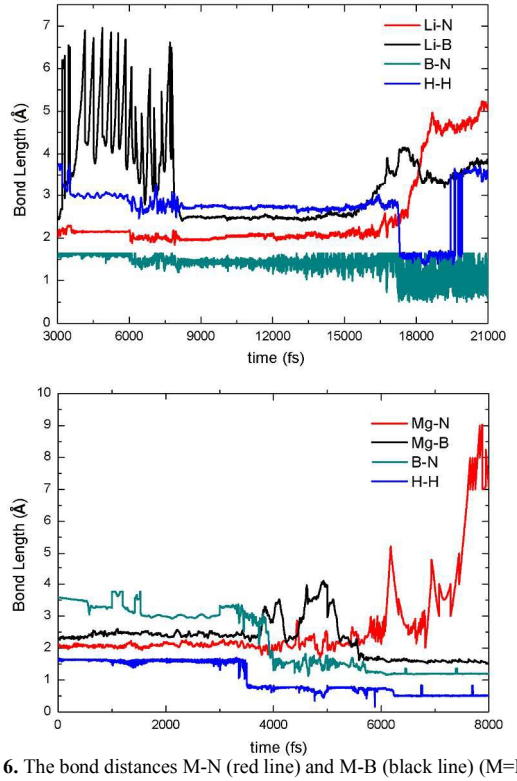

Figure 6. The bond distances M-N (red line) and M-B (black line) (M=Li, Mg) in the decomposition. The green and blue lines mean the shortest bond distances of B-N and H-H.

As for the dehydrogenation of AMgB (Figure S3), the neighboring AMgB starts to polymerize at 3.6595 ps (**TS3'**). Then the first dihydrogen bonds are formed between the hydrogen ions of $[BH_4]^-$and $[NH_3]$ groups (**TS4'-TS6'**) at 3.7995 ps where the bond distances of H-H bonds are 0.764 Å (**TS7'**). Unlike ALB, at the period of 3.6995 – 3.9375 ps in the decomposition of AMgB, no structures of $[NH_2BH_3]$ have been formed after the first dehydrogenation. Both B and N atoms are still bond with the Mg^{2+}, respectively. With increasing the temperature of thermostat, the B-H and N-H bonds vibrate more and more intensive and keep forming dihydrogen bonds as the way of **TS7'**. Until 4 ps, the neighboring B and N atoms begin to get close to each other. At the meantime, part of neighboring $[BH_4]^-$groups polymerize before the formation of **TS8'**. $[Mg(NH_3)_2]^{2+}$ groups generate a large amount of hydrogen cations (at 4.15 ps) while $[BH_4]^+$groups generate hydrogen anions (at 4.6625 ps). So the rest $[NH_3]/[NH_2]^-$ and $[BH_3]/[BH_4]^+$ ions get together to form the intermediates (**TS9'-TS12'**) whose structures similar with DADB or AB [29-30]. There is no doubt that Mg^{2+}catalyzes the formation of hydrogen ion and some time it plays a role of carrier of hydrogen ions (**TS13'** and **TS14'**).The combination of $H^-$and H^+ leads to the continuous dehydrogenation steps after the first one. For the dehydrogenation of AMgB, there is only two steps: Firstly, hydrogen is released from the structures of BH_3-$H^{\delta-}$...$^{+\delta}$H-NH_2. Secondly, hydrogen is released by the interaction of the large amount of hydrogen ions caused by the intensive vibrations of B-H and N-H bonds.

In order to analysis the different variations of structures in the processes, we calculated the bond lengths of M-N and M-B as well as the shortest bond distances of N-B and H-H in Figure 6. The results explain three differences in the decomposition of ALB and AMgB. First of all, all the boron atoms is controllable since the electrostatic interaction between metal and boron except for the decomposition of ALB at high temperature (after 17 ps), which means ALB possibly releases borane or diborane at high temperature. The average bond lengths of Mg-B and Li-B are 2.28 Å and 2.53 Å, respectively. Secondly, the obvious ammonia liberated from ALB at the start of the decomposition where the bond is lengthened as far as to 6.95 Å at 4.885 ps. The intensive oscillations of Li-N bonds are due to the weak polarization of Li^+. AMgB appears the trend to release ammonia at high temperature (after 6 ps, 500 K in the simulation). The bond distances of Mg-N are averaged as 2.19 Å below 500 K theoretically, which is consistent with the previous experiments that AMgB shows excellent dehydrogenation properties[31]. Thirdly, both the results (the blue lines) prove the formation of B-N bonds. For ALB, the bond lengths of B-N are averaged to 1.59 Å to form $[NH_2BH_3]$ groups because of the combination of boron and nitrogen atoms at the period of 17 ps to 20 ps, which just corresponding to the 2nd and 3rd steps of dehydrogenation. For AMgB, the bond distances of B-N bonds are averaged to 1.33 Å means the structures of **TS12'-TS14'** are formed where the nitrogen and boron atoms are hold tightly by Mg^{2+}. The difference is the hydrogen liberation of ALB is mainly from $[NH_2BH_3]$ groups after releasing the first molecular hydrogen. So ALB releases hydrogen at high temperature (280 ºC) rather than ammonia in the experiment[16] because the decomposition of$LiNH_2BH_3$ at high temperature. But for AMgB, hydrogen is formed by H^+ and H^- which is nothing about the structure of $[NH_2BH_3]$. So the second dihydrogen bonds are formed in advance of the formation of B-N bonds in AMgB.

Commonly, the catalysis role of metal cations has been proved in the dehydrogenation and deammoniation. And the reason of the differences in the decomposition is the polarization of the centre metals. The polarization of Mg^{2+} is almost two times than that of Li^+ on the basis of Fajan's rule which make Mg^{2+} bond with nitrogen and boron atoms more stronger. It's the same reason that the dihydrogen bonds are formed between H^+ and H^- in AMgB without the help of $[NH_3]/[NH_2]^-$ and $[BH_3]/[BH_4]^+$groups. Although both ALB and AMgB can not solve the problem of the reversibility of hydrogen storage materials, it is significant for designing of new applicable similar compounds such as metallic hydrazinidoborane. Further investigation is need to understand the reversible decompositions of boron-ammine hydrogen storage material.

Cite this: DOI: 10.1039/c0xx00000x

www.rsc.org/xxxxxx

COMMUNICATION

Notes and references

[a]*Department of Chemistry, Anhui University, Hefei, Anhui 230601, P. R. China. Tel & Fax: +86551 63861279, E-mail: wangkun@ahu.edu.cn*

[b]*State Key Laboratory of Explosion Science and Technology, Beijing Institute of Technology, Beijing 100081 P. R. China. Tel & Fax: +86 10 68918091, E-mail: zjgbit@bit.edu.cn*

[c]*Physical and Theoretical Chemistry Laboratory, University of Oxford, Oxford, OX1 3QR, United Kingdom.*

[d]*State Key Lab of Mechatronics Engineering and Control, Beijing Institute of Technology, Beijing 100081, PR China. E-mail: langxuqiang0536@163.com*

† Electronic Supplementary Information (ESI) available: [details of any supplementary information available should be included here]. See DOI:10.1039/b000000x/

‡ Financial support by National Natural Science Foundation of China (NSFC 20171019) and Doctoral Scientific Research Foundation of Anhui University (J01001955) is acknowledged. It's also should ackowledge the help of Professor John E. McGrady and Dr Vaida Arcisauskaite from Oxford

1. W. Grochala; P. P. Edwards, *Chem Rev* **2004,***104* (3), 1283-1315.
2. P. Kruger, *Int J Hydrogen Energ* **2000,***25*, 1023-1033.
3. S. A. Shevlin; Z. X. Guo, *Chem Soc Rev* **2009,***38* (1), 211-225.
4. U.S. Department of Energy. Development and DemonstrationPlan: Planned Program Activities for 2005–2015, Technical Plan, U.S,**2005**.
5. B.Sakintuna; E. L.Darkrim; M.Hirscher, *Int J Hydrogen Energ* **2007,***32*, 1121-1140.
6. L. F. Brown, *Int J Hydrogen Energ* **2001,***26* (4), 381-397.
7. T. E. Lipman; M. A. Delucchi, *Int J Vehicle Des* **1996,***17*, 562.
8. M. Fleischmann, *J Electroanal Chem* **1989,***261* (2), 301-308.
9. G. Soloveichik; J. H. Her; P. W. Stephens; Y. Gao; J. Rijssenbeek; M. Andrus; J. C. Zhao, *Inorg Chem* **2008,***47* (10), 4290-4298.
10. Q. F. Gu; L. Gao; Y. H. Guo; Y. B. Tan; Z. W.Tang; K. S. Wallwork; F. W. Zhang; X. B. Yu, *Energy Environ. Sci.* **2012,***5*, 7590-7600.
11. U.S. Department of Energy, Preparation and Reactions of Complex Hydrides for Hydrogen Storage: Metal Borohydrides and Aluminum Hydrides. **2009**, 467-471.
12. F. Yuan; Q. F. Gu; Y. H. Guo; W. W. Sun; X. W. Chen; X. B. Yu, *J Mater Chem* **2012,***22*, 1061-1068.
13. F. Yuan; Q. F. Gu; X. W. Chen; Y. B. Tan; Y. H. Guo; X. B. Yu, *Chem Mater* **2012,***24*, 3370-3379.
14. K. Wang; J.-G. Zhang; J.-S. Jiao; T. Zhang; Z.-N. Zhou, *J. Phys. Chem. C* **2014,***118*, 8271-8279.
15. S. R. Johnson; W. I. F. David; D. M. Royse; M. Sommariva; C. Y. Tang; F. P. A. Fabbiani; M. O. Jones; P. P. Edwards, *Chem.–Asian J* **2009,***4*, 849-854.
16. Y. Guo; G. Xia; Y. Zhu; L. Gao; X. Yu, *Chem Commun* **2010,***46*, 2599–2601
17. R. Car; M. Parrinello, *Phys. Rev. Lett.* **1985,***55*, 2471.
18. R. Car; M. Parrinello, *Phys Rev Lett* **1985,***55* (22), 2471-2474.
19. T. D. Kühne; M. Krack; F. R. Mohamed; M. Parrinello, *Phys. Rev. Lett.* **2007,***98* (6), 066401.
20. M. D. Segall; P. J. D. Lindan; M. J. Probert; C. J. Pickard; P. J. Hasnip; S. J. Clark; M. C. Payne, *J. Phys.: Condens. Matter* **2002,***14* (11), 2717.
21. H. J. Monkhorst; J. D. Pack, *Phys. Rev. B* **1976,***13*, 5188-5192.
22. R. AIB, *Trans. Faraday Sco* **1949,***45*, 85-93.
23. J. P. Perdew; Y. Wang, *Phys. Rev. B* **1992,***45*, 13244-3249.
24. J. P. Perdew; K. Burke; M. Ernzerhof, *Phys. Rev. Lett.* **1996,***77*, 3865-3868.
25. D. Vanderbilt, *Phys. Rev. B* **1990,***41* (11), 7892-7895.
26. T. H. Fischer; J. Almlof, *J. Phys. Chem.* **1992,***96* (24), 9768-9774.
27. N. S, *Mol. Phys* **1984,***52*, 255-268.
28. K. Wang; J. Zhang; T. Zhang, *International Journal of Hydrogen Energy* **2014,***39*, 21372-21379.
29. K. Wang; J.-G. Zhang; T.-T. Man; M. Wu; C.-C. Chen, *Chem. Asian J.* **2013,***8*, 1076 - 1089.
30. S. A. Shevlin; B. Kerkeni; Z. X. Guo, *Phys Chem Chem Phys* **2011,***13* (17), 7649-7659.
31. Y. Yang; Y. Liu; Y. Li; M. Gao; H. Pan, *Chem. Asian J.* **2013,***8*, 476 - 481.

Graphic abstract

The dehydrogenation processes of ammine metallic borohydrides can be controlled if we choose appropriate centre metals.